Journal of Biomolecular Screening
http://jbx.sagepub.com/

High-Throughput Fluorescence Assay for Small-Molecule Inhibitors of Autophagins/Atg4

Chih-Wen Shu, Charitha Madiraju, Dayong Zhai, Kate Welsh, Paul Diaz, Eduard Sergienko, Renata Sano and John C. Reed

J Biomol Screen published online 18 January 2011
DOI: 10.1177/1087057110392996

The online version of this article can be found at:
http://jbx.sagepub.com/content/early/2011/01/14/1087057110392996

Published by:
SAGE
http://www.sagepublications.com

High-Throughput Fluorescence Assay for Small-Molecule Inhibitors of Autophagins/Atg4

CHIH-WEN SHU, CHARITHA MADIRAJU, DAYONG ZHAI, KATE WELSH, PAUL DIAZ, EDUARD SERGIENKO, RENATA SANO, and JOHN C. REED

Autophagy is an evolutionarily conserved process for catabolizing damaged proteins and organelles in a lysosome-dependent manner. Dysregulation of autophagy may cause various diseases, such as cancer and neurodegeneration. However, the relevance of autophagy to diseases remains controversial because of the limited availability of chemical modulators. Herein, the authors developed a fluorescence-based assay for measuring activity of the autophagy protease, autophagin-1(Atg4B). The assay employs a novel reporter substrate of Atg4B composed of a natural substrate (LC3B) fused to an assayable enzyme (PLA_2) that becomes active upon cleavage by this cysteine protease. A high-throughput screening (HTS) assay was validated with excellent Z′ factor (>0.7), remaining robust for more than 5 h and suitable for screening of large chemical libraries. The HTS assay was validated by performing pilot screens with 2 small collections of compounds enriched in bioactive molecules (n = 1280 for Lopac™ and 2000 for Spectrum™ library), yielding confirmed hit rates of 0.23% and 0.70%, respectively. As counterscreens, PLA_2 and caspase-3 assays were employed to eliminate nonspecific inhibitors. In conclusion, the LC3B-PLA_2 reporter assay provides a platform for compound library screening for identification and characterization of Atg4B-specific inhibitors that may be useful as tools for interrogating the role of autophagy in disease models. (*Journal of Biomolecular Screening* XXXX;xx-xx:xx)

Key words: autophagy, Atg4, autophagin, high-throughput screening, protease

INTRODUCTION

AUTOPHAGY IS AN EVOLUTIONARILY CONSERVED PROCESS whereby cells catabolize damaged proteins and organelles for purposes of generating substrates for sustaining adenosine triphosphate (ATP) production during times of nutrient deprivation.[1,2] Three types of autophagy have been described based primarily on cellular morphology considerations, including macroautophagy, microautophagy, and chaperone-mediated autophagy.[3] For the most part, autophagy-related genes (Atg) are required for these 3 forms of autophagy, with some minor difference.[4,5] The genes responsible for autophagy have been identified, largely through genetic analysis of yeast, *Saccharomyces cerevisiae*, and are conserved in mammals, plants, and essentially all eukaryotes.[6]

Roles for autophagy have been suggested in either causation or prevention of disease. For example, autophagy has been implicated in eliminating senescent and insoluble proteins that are not degraded via proteasome-based mechanisms, representing an important "housekeeping" function for some types of cells, such as neurons, where it may be helpful for preventing protein inclusion body diseases associated with neurodegeneration.[7,8] Autophagy also plays helpful roles in the context of host-pathogen interactions, where autophagic vesicles help to surround intracellular virus particles and bacteria, targeting them for lysosomal destruction.[9,10] In contrast, autophagy may promote the pathogenesis and progression of tumors, allowing cancer cells to survive nutrient-poor and hypoxic environments—such as those found in the centers of rapidly growing malignant lesions that have outstripped their vascular supply.[11] Conversely, some components of the autophagy machinery have also been reported to be required for nonapoptotic cell death, suggesting the concept of autophagic cell death.[12] Altogether, the role of autophagy in disease remains largely controversial.

Chemical inhibitors of autophagy are essentially nonexistent, with the few agents available for aiding research. The compound 3-methyladenine (3-MA) has been touted as an autophagy inhibitor but requires millimolar concentrations to inhibit class III phosphatidyl inositol kinases (PI3Ks) involved in autophagy.[13] Bafilomycin A1 is also commonly employed for suppressing autophagic flux due to its inhibition of the vacuolar

Sanford-Burnham Medical Research Institute, Program on Apoptosis and Cell Death Research, and Conrad Prebys Center for Chemical Genomics, La Jolla, CA, USA.

Received Jul 28, 2010, and in revised form Oct 22, 2010. Accepted for publication Oct 25, 2010.

Supplementary material for this article is available on the *Journal of Biomolecular Screening* Web site at http://jbx.sagepub.com/supplemental.

Journal of Biomolecular Screening XX(X); XXXX
DOI: 10.1177/1087057110392996

type H^+-ATPase (V-ATPase), blocking acidification of lysosomes and endosomes. However, long-term treatment (>4 h) of cells with bafilomycin A1 also interferes the trafficking of proteosomes, endosomes, and other cellular processes.[14,15] A need therefore exists for chemicals that target specific components of the autophagy machinery for use as research tools for addressing questions about autophagy mechanisms and investigating the role of autophagy in diseases.

Autophagins are a class of cytosolic cysteine proteases required for autophagy.[16] Autophagins cleave Atg8 to promote its conjugation with phosphatidylethanolamine (PE) in the membranes of autophagic vesicles by a ubiquitin-like system, which is required for autophagosome formation and participates in targeting these vesicles to lysosomes for fusion and degradation of their contents.[17] Autophagins also promote deconjugation of Atg8-PE to liberate Atg8 from membrane at or before the final stage of fusion between autophagosome and lysosomes, suggesting that deconjugation of Atg8-PE is required for the fusion.[18] The human genome contains 4 independent genes encoding the Atg4 orthologs (termed *autophagins*), including Atg4A/autophagin-2, Atg4B/autophagin-1, 4C/autophagin-3, and 4D/autophagin-4.[16] Atg4B cleaves most of human Atg8 homologs in vitro, including (1) microtubule-associated light chain 3 (LC3; which has A, B, and C isoforms), (2) GABA(A) receptor–associated protein-like 1 (GABARAP-L1), (3) GABA(A) receptor–associated protein (GABARAP), and (4) Golgi-associated ATPase enhancer of 16 kDa (GATE-16, also known as GABA(A) receptor–associated protein-like 2).[19-21] In contrast, Atg4A has activity mainly for GATE-16 in vitro.[22] Atg4B knockout mice show reduction of proteolysis of all Atg8 homologs except GATE-16, suggesting that Atg4A compensates for cleavage of GATE-16 in Atg4B knockout mice.[21] By comparison, Atg4C and Atg4D show minor protease activity or require posttranslational modification (caspase-3 cleavage) for activation,[20,23] indicating Atg4B is functionally dominant in the regulation of autophagy.

In this study, we have selected autophagin-1/Atg4B as a target for developing novel inhibitors of autophagy. We devised a Atg4B high-throughput screening (HTS) assay using a LC3B-PLA_2 reporter substrate (Shu, 2010 #16880) in 384-well format that has excellent performance characteristics (Z′ factor >0.7) and verified by pilot library screening and counterscreens that the assay is suitable for HTS of chemical libraries.

EXPERIMENTAL PROCEDURES

Plasmid constructions

Plasmids for bacterial expression of autophagin-1 (Atg4B) and substrate protein LC3B were constructed as previously described.[19] Briefly, PCR products were cloned into bacterial expression vector pETDuet-1 (Novagen, San Diego, CA) in frame with an N-terminal His tag. The mature human phospholipase A_2 (PLA_2) group X G10 (amino acids 43-165) was amplified from a human fetal brain cDNA library (Open Biosystems, San Diego, CA) and fused with LC3B in pETDuet-1. Site-directed mutagenesis of Atg4B C74A or LC3B G120A was carried out by the QuickChange kit according to the manufacturer's instructions (Stratagene, La Jolla, CA).

Protein expression and purification in Escherichia coli

Atg4B or catalytic mutant Atg4B C74A expression plasmid was transformed into *Escherichia coli* BL21 (DE3; Invitrogen, San Diego, CA). Protein expression was induced by 0.1 mM isopropyl β-D-1-thiogalactopyranoside (IPTG; Invitrogen) at 15°C for 6 h. His_6-tagged proteins were purified using Ni-NTA-agarose (Qiagen, Valencia, CA) and eluted with a 20- to 250-mM imidazole gradient in 20 mM Tris (pH 8.0), 150 mM NaCl, and 10 mM β-mercaptoethanol.

His_6-tagged LC3B-PLA_2 protein was induced by 1 mM IPTG at 37°C for 4 h to obtain inclusion bodies. The inclusion bodies were solubilized with 20 mM Tris buffer (pH 8.0) containing 0.5 M NaCl, 5 mM imidazole, 6 M guanidine hydrochloride, and 1 mM β-mercaptoethanol and loaded into the Ni-NTA column. The denatured proteins were refolded with refolding buffer (20 mM Tris [pH 8.0], 0.5 M NaCl, 20 mM imidazole, 1 mM β-mercaptoethanol) in the presence of linear 6-0 M gradient urea. The refolded proteins were eluted with a 20- to 500-mM gradient imidazole in 20 mM Tris (pH 8.0), 150 mM NaCl, and 10 mM β-mercaptoethanol.

For production of active PLA_2 protein, LC3B-PLA_2 fusion protein (2.5 μM) was incubated with Atg4B (100 nM) in PLA_2 reaction buffer (20 mM Tris-HCl [pH 8.0], 2 mM $CaCl_2$, and 1 mM dithiothreitol [DTT]) at room temperate for 16 h. The cleaved PLA_2 protein was purified with Ni-NTA column (Qiagen) to remove His_6-tagged LC3B and Atg4B. Caspase-3 protein was purified as described previously.[24,25]

Atg4B cleavage of synthetic protein substrates

Atg4B (wild-type [WT]) or catalytic mutant Atg4B C74A was incubated with 400 nM protein substrates in a 50-μL reaction buffer containing 50 mM Tris (pH 8.0), 150 mM NaCl, and 1 mM DTT at 37°C for 1 h. Reactions were stopped by addition of 50 μL of 2× Laemmli sodium dodecyl sulfate (SDS) sample and subjected to 13% SDS–polyacrylamide gel electrophoresis (PAGE) followed by GelCode Blue staining (Thermo Fisher Scientific, Asheville, NC) or transfer to nitrocellulose membranes (Sigma-Aldrich, St. Louis, MO) for immunoblotting analysis using anti-myc antibody (Roche, Indianapolis, IN). Proteins were detected using peroxidase-conjugated antimouse IgG secondary antibody by Super Signal and chemiluminescence substrate (Pierce, Rockford, IL) with exposure to X-ray film.

Atg4B activity measured using LC3B-PLA_2 substrate

The assay was modified from a previous report.[26] Briefly, recombinant Atg4B was mixed with LC3B-PLA_2 fusion protein

to a final volume of 20 μL PLA_2 reaction buffer (20 mM Tris-HCl [pH 8.0], 2 mM $CaCl_2$, and 1 mM DTT) containing 20 μM 2-(6-(7-nitrobenz-2-oxa-1,3-diazol-4-yl)amino) hexanoyl-1-hexadecanoyl-sn-glycero-3-phosphocholine (NBD-C_6-HPC) (Invitrogen) in wells of black-walled 384-well plates (Greiner Bio-One, Frickenhausen, Germany). Fluorescence intensity was measured for various times using an Analyst™ HT (Molecular Devices, Sunnyvale, CA) at room temperature with excitation and emission wavelengths of 485 and 530, respectively. Data were analyzed by GraphPad Prism software (GraphPad Software, San Diego, CA). To determine robustness of the assay, Z′ factor was calculated as a defined equation: $1 - 3(SD_{+Atg4B} + SD_{-Atg4B})/mean_{+Atg4B} - mean_{-Atg4B}$, where SD is the standard derivation of signal for both positive ($_{+Atg4B}$) and negative ($_{-Atg4B}$) controls.[27]

High-throughput screening

For HTS, 20 nL of each compound (10 mM in DMSO) of 1280 compounds from the LOPAC™ library (Sigma-Aldrich) or 2000 compounds from the Spectrum™ library (Spectrum Chemicals & Laboratory Products, Gardena, CA) were plated into black 384-well, round-well plates using a Labcyte Echo 550 acoustic pipetter (Agilent Technologies, Wilmington, DE). Recombinant Atg4B (0.2 nM, 10 μL) was dispensed to each well using ThermoScientific Matrix WellMate bulk dispenser (Thermo Fisher Scientific). LC3B-PLA_2 fusion protein (50 nM, 10 μL) diluted in 2× PLA_2 reaction buffer (40 mM Tris-HCl [pH 8.0], 4 mM $CaCl_2$, and 2 mM DTT) containing 40 μM NBD-C_6-HPC (Invitrogen) was then added to each well. Fluorescence intensity was measured within 30 to 60 min using an Analyst™ HT (Molecular Devices) at room temperature with excitation and emission wavelengths of 485 and 530, respectively. The inhibition of compounds was recorded as percentage compared to DMSO control. Twofold serial dilutions (maximal final concentration 100 μM) of compounds were used for determination of dose-responsive curves. IC_{50} values were calculated by nonlinear regression analysis employing GraphPad Prism software (GraphPad Software).

Counterscreens for PLA_2 and caspase-3 assay

For the PLA_2 assay, 20 nL of each hit (10 mM in DMSO) from LOPAC™ or Spectrum™ libraries was plated into black 384-well, round-well plates using a Labcyte Echo 550 acoustic pipetter (Agilent Technologies). Active PLA_2 (500 nM, 10 μL) was dispensed to each well, then mixed with NBD-C_6-HPC (Invitrogen; 20 μM, 10 μL) in PLA_2 reaction buffer at room temperature for 2 h. Fluorescence intensity was measured with excitation and emission wavelengths of 485 and 530, respectively. Caspase-3 assay was determined using methods modified from a previous report.[25] Briefly, His_6-tagged caspase-3 (1 nM, 10 μL) was mixed with acetyl-Asp-Glu-Val-Asp-AFC (200 μM, 10 μL) in assay buffer (50 mM HEPES [pH 7.4], 10% sucrose, 1 mM EDTA, 0.1% 3-[(3-cholamidopropyl)dimethylammonio]-1-propanesulfonate [CHAPS], 100 mM NaCl, and 1 mM DTT) in wells of white 384-well plates containing 20 nL hit compound (10 mM in DMSO). Fluorogenic AFC product was measured at 37°C for 1 h with excitation and emission wavelengths of 405 and 510, respectively.

RESULTS

Development of Atg4B assay based on LC3B-PLA_2 fusion protein substrate

To develop a primary HTS assay for autophagins, we generated an expression plasmid for production of LC3B-PLA_2 fusion protein (*substrate*) in bacteria. The enzyme phospholipase A_2 (PLA_2) is inactive when expressed as a fusion protein with polypeptide appendages added to its N-terminus (**Fig. 1A**).[28] LC3B is among the endogenous substrates of autophagin-1/Atg4B. Thus, we generated a novel substrate for autophagin screening by producing a recombinant LC3B-PLA_2 fusion protein, such that Atg4-mediated cleavage of LC3B liberates active PLA_2 (Shu, 2010 #16880). Using bacterially expressed, purified His_6-Atg4B (*protease*), we determined that cleavage of LC3B-PLA_2 by Atg4B is done in a concentration-dependent manner, as shown by monitoring cleavage products by SDS-PAGE with protein stains or immunoblotting (**Fig. 1B**). Moreover, cleavage of the LC3B-PLA_2 substrate was not observed with an Atg4B catalytic mutant (Cys/Ala). Importantly, NBD fluorescence release from the PLA_2 substrate NBD-C_6-HPC also increased in a concentration-dependent manner, as measured in a plate reader assay (**Fig. 1C**).

We also explored the reactivity of Atg4B on a mutant of LC3B-PLA_2 in which the glycine residues at which LC3B cleavage normally occurs was converted to alanine. Atg4B only slightly cleaved the LC3B-PLA_2 (Gly/Ala) mutant as measured by generation of PLA_2 activity (**Fig. 1B**). We presume that the PLA_2 activity generated from exposure of the mutant substrate to Atg4B may be due to cleavage at a glycine residue provided by PLA_2 because glycine is the first reside in PLA_2 where fusion to LC3B occurred (the wild-type junction sequence is ETF**G**GILE, where bold indicates the site of cleavage, and the mutant sequence is ETF**A**GILE).

To determine the optimal concentration of Atg4B and LC3B-PLA_2 for the assay, the concentration of Atg4B was titrated by 2-fold serial dilution from 1250 to 0 pM (**Fig. 2A**). Atg4B-mediated increase of fluorescence in LC3B-PLA_2 containing reactions was observed in a time- and concentration-dependent manner. Similar to prior reports using ubiquitin-PLA_2 for assays[26] of deubiquiteness, a kinetic lag effect was observed at low concentrations of Atg4B (<160 pM), which has been attributed to PLA_2 substrate NBD-C_6-HPC-forming micelles. Next, LC3B-PLA_2 was 2-fold serial diluted from 200 to 0 nM for assessing optimal substrate concentration (**Fig. 2B**), showing the apparent K_m is approximately 25 nM.

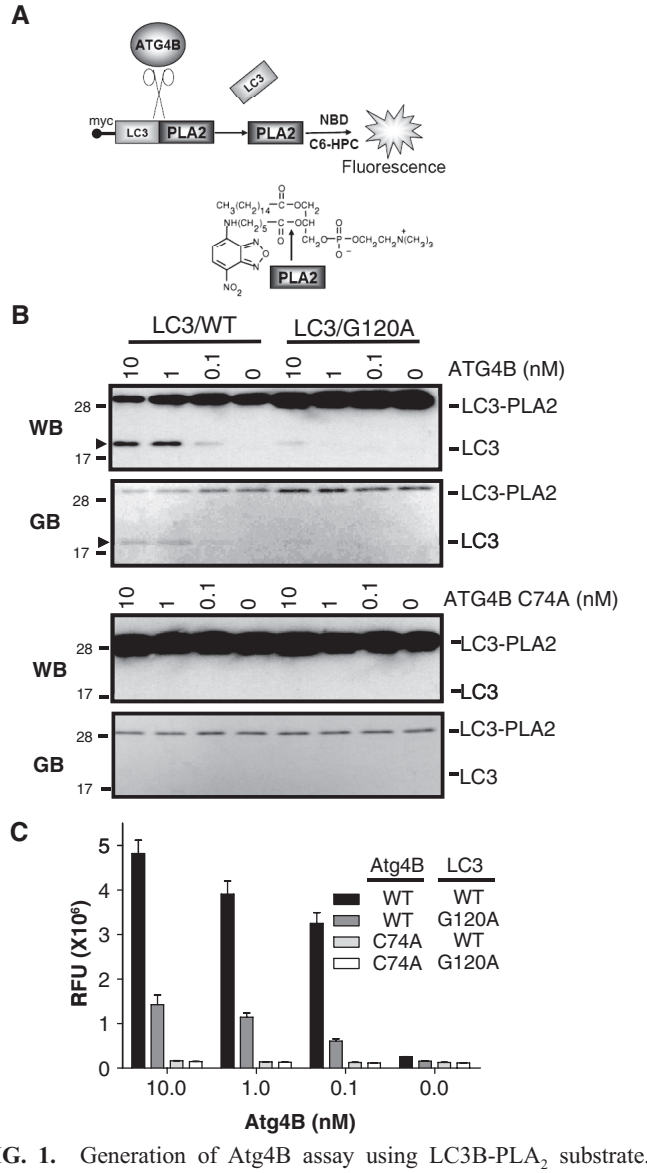

FIG. 1. Generation of Atg4B assay using LC3B-PLA_2 substrate. (**A**) Scheme depicting basis for the LC3B-PLA_2 substrate for monitoring Atg4B activity. Atg4B cleaves the Gly120 site of proLC3B to release catalytically active PLA_2, which hydrolyzes NBD-C_6-HPC, generating fluorescence. (**B**) Tenfold serial dilutions of 10 nM Atg4B wild-type (top panel) or catalytic mutant (bottom panel) were incubated with 400 nM LC3B-PLA_2 wild-type or cleavage site mutant (G120A) fusion proteins at 37°C for 1 h. Cleavage of LC3B-PLA_2 proteins was determined by SDS-PAGE with immunoblotting (WB) or GelCode Blue staining (GB). Arrowheads indicate cleavage product. (**C**) Tenfold serial dilutions of Atg4B wild-type or catalytic mutant (maximal final concentration 10 nM) were incubated with 100 nM LC3B-PLA_2 wild-type or cleavage site mutant (G120A) fusion proteins in PLA_2 reaction buffer (20 mM Tris-HCl [pH 8.0], 2 mM $CaCl_2$, and 1 mM dithiothreitol) containing 20 μM NBD-C_6-HPC at room temperature for 30 min. PLA_2 activity was monitored by hydrolysis of NBD-C_6-HPC, measuring fluorescence with excitation and emission filters of 485 nm and 530 nm, respectively, and reporting results as relative fluorescence units (RFU). Data represent the mean ± SD of 4 experiments.

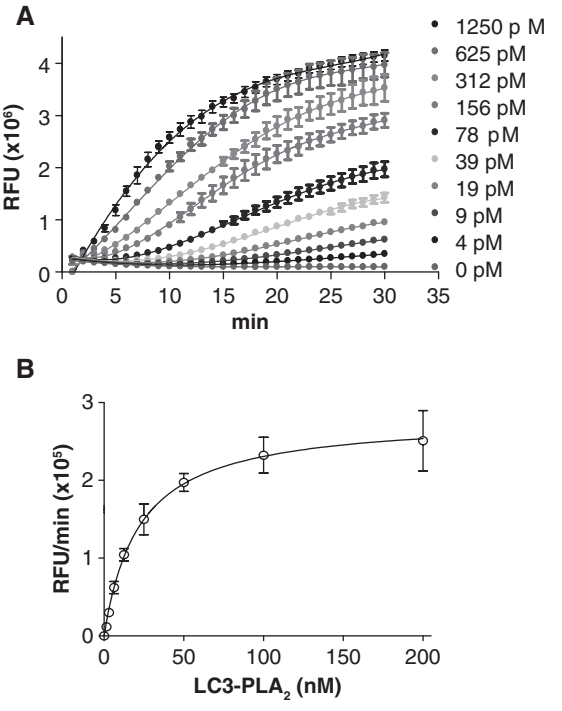

FIG. 2. Determination of optimal concentrations of Atg4B and LC3B-PLA_2 for the high-throughput screening assay. (**A**) Twofold serial dilutions of Atg4B (maximal final concentration 1250 pM) were mixed with 100 nM LC3B-PLA_2 to a final volume of 20 μL in wells of black-walled 384-well plates at room temperature. PLA_2 activity was monitored by hydrolysis of NBD-C_6-HPC, measuring fluorescence with excitation and emission filters of 485 nm and 530 nm, respectively. Data represent enzyme progress curves, showing relative fluorescence units (RFU) generated over time. (**B**) Twofold serial dilutions of LC3B-PLA_2 (maximal final concentration 200 nM) were incubated with 0.1 nM Atg4B in the PLA_2 reaction buffer at final volume of 20 μL in 384-well plates at room temperature for 30 min. The rate of PLA_2 activity generation was measured (RFU/min). Data processing was performed using nonlinear regression analysis employing GraphPad Prism software. Data represent the mean ± SD of 4 experiments.

HTS implementation of the LC3B-PLA_2 reporter assay for Atg4B

To study assay performance for the HTS environment, the Atg4B assay was tested in 384-well plates using 96 wells each of (a) the negative control (without Atg4B); (b) the positive control (Atg4B without inhibitors); (c) a control for protease inhibition (Atg4B with general cysteine protease inhibitor N-ethylmaleimide (10 mM), which covalently modifies the active site cysteine of proteases; and (d) EGTA (5 mM), a chelator of calcium, which is essential for PLA_2 activity (**Fig. 3**). For this experiment, LC3B-PLA_2 was employed at 25 nM and protein at 0.1 nM, based on the results from the dose-response analysis. Fluorescent intensity was measured for up to 5 h (**Fig. 3B**). The Z′ statistic was calculated from the data and

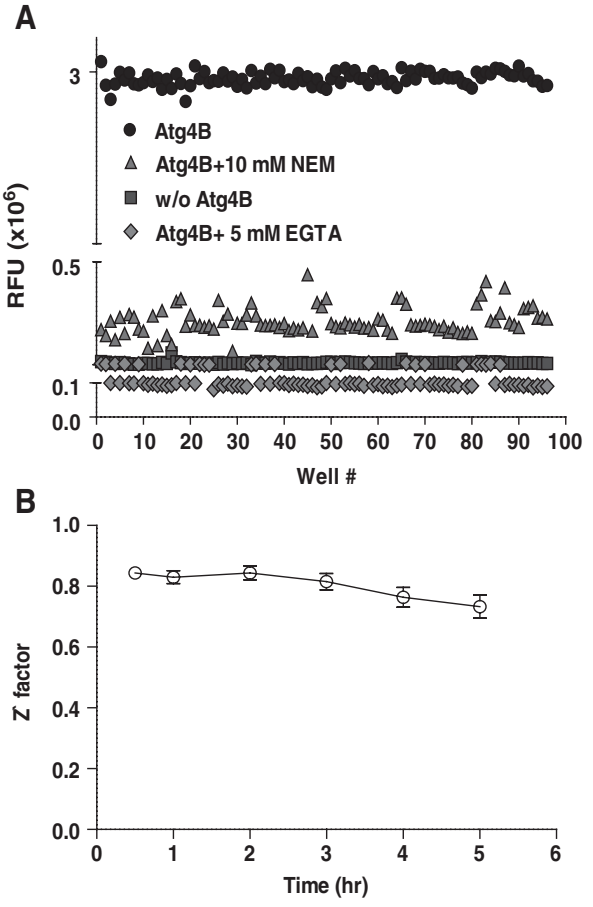

FIG. 3. Characterization of LC3B-PLA_2 reporter assay for high-throughput screening. (**A**) LC3B-PLA_2 (25 nM) was incubated without (squares) or with (circles) Atg4B (0.1 nM) in the absence or presence of calcium chelator, EGTA (5 mM) (diamonds), or general cysteine protease inhibitor, N-ethylmaleimide (10 mM) (triangles), in PLA_2 reaction buffer (20 mM Tris-HCl [pH 8.0], 2 mM $CaCl_2$, and 1 mM dithiothreitol) containing 20 μM NBD-C_6-HPC for 0.5 h using 96 replicate wells of 384-well plates for each condition. PLA_2 activity was measured by fluorescence intensity with excitation and emission filters of 485 nm and 530 nm, respectively, and reporting results as relative fluorescence units (RFU). (**B**) The Z′ factor was calculated according to positive control (with Atg4B) and negative control (without Atg4B) over time, from 0.5 to 5 h.

determined to be >0.7 when measured from 0.5 to 5 h. Thus, the assay exhibits performance characteristics sufficient for use in HTS with robust performance for at least 5 h after preparing reactions in microwells.

Screening and characterization of hits from the LOPAC™ and Spectrum™ libraries

Next, we undertook a pilot screen of a chemical library (LOPAC™) enriched in bioactive molecules to test the performance of the HTS assay (**Fig. 4A**). The compound library was screened at an average compound concentration of approximately 10 μM at room temperature for 1 h, which is within the linear range of the HTS assay. The assays contained 0.1% DMSO final volume. From this screen of 1280 chemical compounds, we obtained 4 hits (cut-off of 50% inhibition). The hits were cherry picked and retested at the screening concentration. Of these, 3 hits were confirmed, constituting a hit rate of 0.23% (see **Supplemental Figure S1A**). One of the hit compounds (A1895) has been found previously by us to inhibit GAPDH and UBC13 (data not shown), which are both enzymes that contain cysteine in their active sites, suggesting that this compound is nonselective. The remaining 2 hits from HTS were first filtered with a PLA_2 counterscreen assay to eliminate compounds directly inhibiting PLA_2 or interfering with fluorescence (see **Supplemental Figure S1B**). Neither of the hits directly inhibited PLA_2. Next, hits were also evaluated using a counterscreen assay for caspase-3, another class of cysteine protease, to eliminate redox-active compounds that attack cysteine within the catalytic centers of enzymes (see **Supplemental Figure S1C**). Both of the remaining compounds inhibited caspase-3, indicating that they are nonselective. Although no promising hits were obtained from the LOPAC™ library, the conditions used for library screening provided a reasonable hit rate.

We therefore also screened the Spectrum™ library, which consists of 2000 bioactive compounds. Again, the HTS assay was performed at room temperature for 1 h. After screening and confirmation, 14 of initial 25 hits were confirmed, thus representing a confirmed hit rate of 0.7% (**Fig. 4B,C**). The hits were evaluated with 2 counterscreens: PLA_2 and caspase-3. Inhibitor controls for the counterscreen assays included EGTA (5 mM, PLA_2 assay) and zVAD-fmk (10 μM, caspase-3 assay) (**Fig. 4D,E**). The Z′ factors were 0.78 and 0.60 for the PLA_2 and caspase-3 assay, respectively. Only 1 of the 14 confirmed hits showed inhibitory activity in the PLA_2 counterscreen assay, indicating that it was a false positive (**Fig. 4D**). None of the hits inhibited caspase-3 activity (**Fig. 4E**).

We also tested the hits with LCB-PLA_2 reporter assay in kinetic mode using covalent inhibitor iodoacetamide (IAA) as a positive control, which attacks the active site cysteine of Atg4B (see **Supplemental Figure S2**). Each of the hits reduced the slope of the enzyme progress curves, showing slower but linear rates of substrate hydrolysis. Finally, the hits were tested using our autophagin-1 HTS assay with or without DTT to identify redox-active compounds that generate superoxide and thus oxidize cysteines in target proteins.[29,30] Two of the compounds (1504078 and 1504080) showed additive inhibition in the presence of DTT and thus are likely to inhibit in vitro through a redox-based mechanism (see **Supplemental Figure S3**).

The hits were then cherry picked for dose-response testing (**Table 1**). Of the 13 remaining hits, 4 inhibited Atg4B with IC_{50} <10 μM, showing concentration-dependent inhibition with well-fitted curves using the Hill equation ($0.5 \leq H \leq 1.5$,

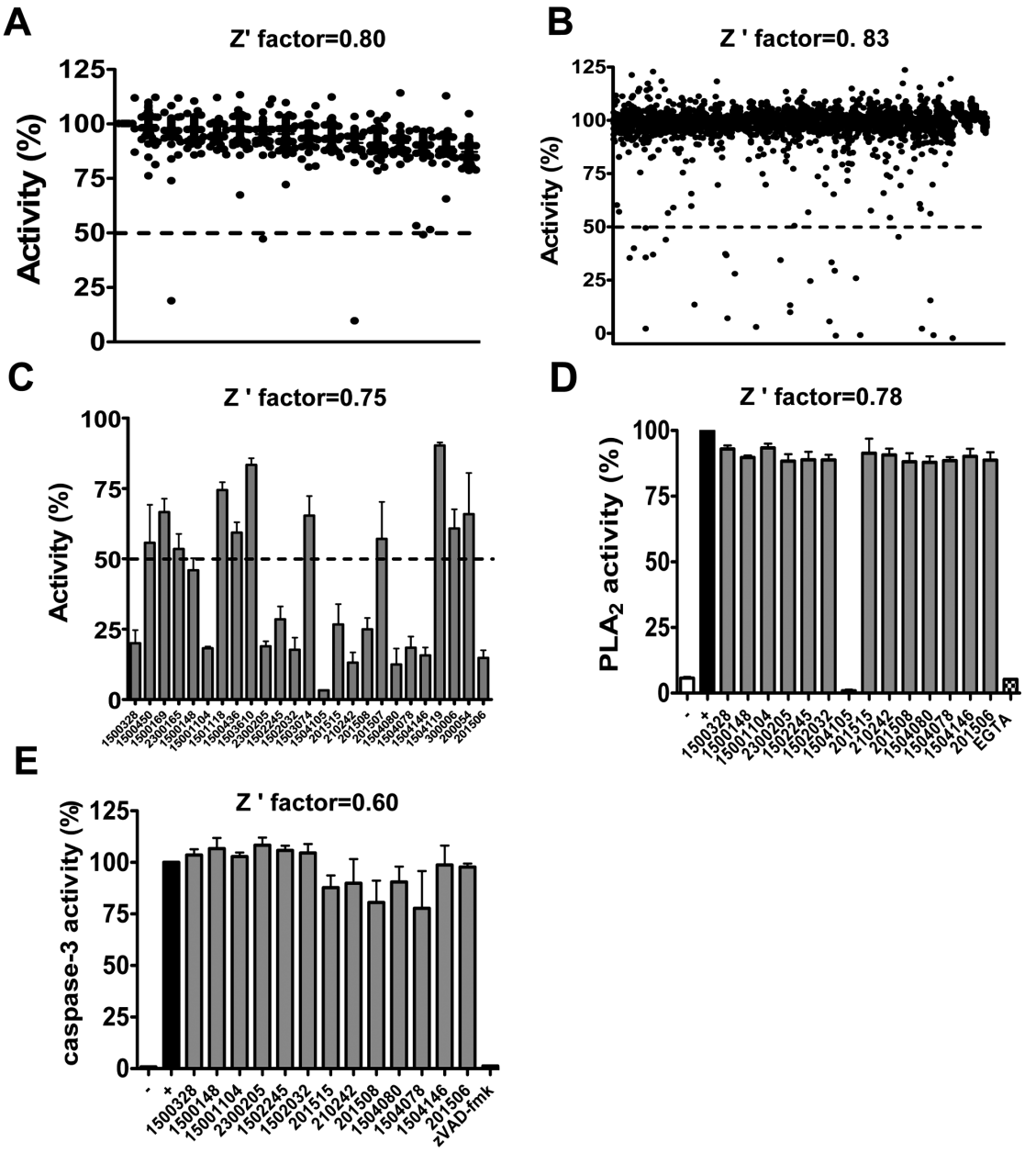

FIG. 4. High-throughput screening (HTS) for Atg4B inhibitors—pilot library screens. (**A**) LC3B-PLA_2 (25 nM) was mixed with Atg4B (0.1 nM) in PLA_2 reaction buffer containing 20 μM NBD-C_6-HPC on ice, and then 20-μL aliquots were dispensed into wells of a 384-well plate containing compounds (10 μM average approximate concentration) of the LOPAC™ collection for 1 h. PLA_2 activity was measured as a percentage relative to control wells that received DMSO only. Z′ factor was calculated by including a row of wells without Atg4B as a negative control (assay minimum) and a row of wells with Atg4B without compounds (DMSO only) as positive control (assay maximum). The 50% inhibition cut-off used for hit calling is indicated. (**B**) Assays were performed as in **A** using the Spectrum™ library. (**C**) LC3B-PLA_2 (25 nM) and Atg4B (0.1 nM) were mixed with hits from HTS using the Spectrum™ library in PLA_2 reaction buffer (20 mM Tris-HCl [pH 8.0], 2 mM $CaCl_2$, and 1 mM dithiothreitol) containing 20 μM NBD-C_6-HPC for 1 h. The PLA_2 activity was measured as percentage compared to positive control (Atg4B alone). (**D**) The confirmed hits were mixed with active PLA_2 (250 nM) assay in the reaction buffer containing 20 μM NBD-C_6-HPC at room temperature for 2 h to eliminate the compound directly inhibiting PLA_2 or interfering with fluorescence. The PLA_2 activity was measured as a percentage compared to the positive control (PLA_2 alone). EGTA (5 mM) was used as control for inhibiting PLA_2 activity. (**E**) The confirmed hits were mixed with caspase-3 (0.5 nM) in assay buffer containing Ac-DEVD-AFC (100 μM) at 37°C for 1 h. The activity of caspase-3 was measured by AFC fluorescence with excitation and emission filters of 400 nm and 505 nm, respectively, reporting results as a percentage compared to positive control (+, caspase-3 alone). zVAD-fmk (10 μM) was used for inhibiting caspase-3 activity.

Table 1. IC_{50} Determination for Screening Hits Using the LC3B-PLA_2-Based Assay

Compound ID	*IC_{50}*	*Hill Slope*
1500328	11.1	1.2
1500148	13.7	0.8
1501104	2.0	1.7
2300205	22.0	1.7
1502245	5.5	1.2
1502032	10.1	1.0
201515	8.5	4.8
201508	2.3	1.0
1504080	1.1	1.4
1504078	1.7	1.2
201506	11.3	1.8
210242	5.6	2.4
1504146	12.3	0.7

Reactions containing Atg4B (0.1 nM) and LC3B-PLA_2 (25 nM) were incubated with 2-fold serial dilutions of 14 screening hits (maximum final concentration 100 μM) obtained from the Spectrum™ library. Estimated IC_{50} values and Hill slopes for each hit were determined. Data are mean of triplicate determinations.

$r^2 > 0.9$; **Fig. 5**). The IC_{50} of compounds 201508, 1502245, 1504078, and 1504080 was estimated at 2.3, 5.5, 1.7, and 1.1 μM (mean ± SEM), respectively. Taken together, our HTS assay provides the first platform for screening chemical libraries for autophagin inhibitors.

DISCUSSION

Autophagins play a crucial role in conjugation and deconjugation of Atg8 paralogs to autophagic vesicles and are indispensable for the process of autophagy.[31] Chemical inhibitors of autophagy are largely lacking, thus representing a void in the armamentarium of experimental approaches available to study this process. In this study, we have devised an HTS fluorogenic assay for measuring activity of autophagin-1 (Atg4B). The assay performs robustly in the 384-well environment with Z′ factors consistently >0.7. The signal-to-noise ratio and reproducibility of the assay are sustained for at least 5 h, which is appropriate for HTS applications. Moreover, acceptable hit rates were obtained in pilot screens of 3280 bioactive compounds at ~10 μM, with confirmed hit rates of 0.23% to 0.70%. Finally, the expression plasmids and methods for bacterial expression that we have described for recombinant Atg4B (*protease*) and LC3B-PLA_2 (*substrate*) proteins provide excellent yields (~6 mg/L culture), thus making large-scale chemical library screening entirely feasible.

PLA_2 has been used previously in other protease applications because of the inhibitory effect that N-terminal appendages have on this enzyme.[26] When expressed as a fusion protein with a cleavable N-terminus, PLA_2 serves as a convenient reporter for monitoring protease activity. For example, ubiquitin-PLA_2 fusion protein is cleaved by deubiquitin enzymes (DUBs) and efficiently

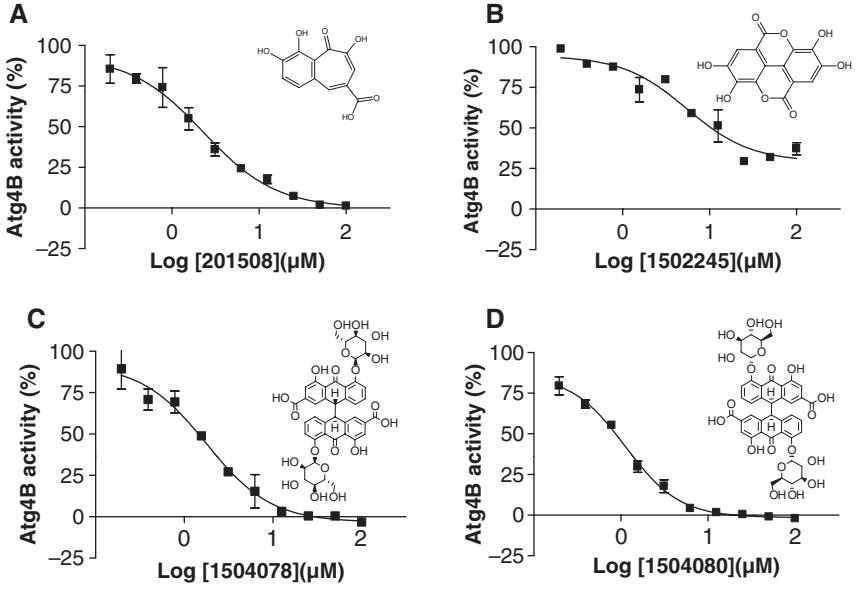

FIG. 5. Dose-dependent inhibition of Atg4B by screening hits. Reactions containing Atg4B (0.1 nM) and LC3B-PLA_2 (25 nM) were incubated with 2-fold serial dilutions of screening hits (maximum final concentration 100 μM), including (**A**) 201508, (**B**) 1502245, (**C**) 1504078, and (**D**) 1504080. Fluorescence was measured with excitation and emission filters of 485 nm and 530 nm, respectively, and reporting results as a percentage of control activity for reactions receiving only DMSO. The estimated IC_{50} values are 2.3, 3.0, 1.7, and 1.1 μM for compounds 201508, 1504105, 1504078, and 1504080, respectively, compared to positive control (DMSO). Representative graphs are shown. Data are mean ± SEM of triplicate determinations. The structure of hits is shown in each panel.

produces active PLA_2. The LC3B-PLA_2 fusion protein substrate that we have recently described and characterized represents the first application of the PLA_2 fusion protein approach to autophagy proteases.[19] Compared to AFC (7-amino-4-trifluoromethyl coumarin)–conjugated tetrapeptide substrates that we investigated in a previous study,[19] the catalytic efficiency of the LC3B-PLA_2 substrate is 5.7×10^5 higher (k_{cat}/K_m 5.26×10^5 M^{-1}/s^{-1}). In this regard, the crystal structure of the LC3/Atg4B complex has shown that full-length LC3B induces conformational changes in Atg4B that promote formation of the active catalytic site,[32] thus presumably explaining why our LC3B-PLA_2 protein substrate is far superior to peptide substrates. Thus, the LC3B-PLA_2 substrate is not only more physiological but is also much more efficient from the perspective of enzyme kinetics.

We have also begun to create additional PLA_2 fusion proteins with other autophagin substrates appended, including GATE-16 and GABARAP-L1, which can serve as alternatives to LC3B-PLA_2 for some autophagins or as secondary assay reagents for independent confirmation of hits. In this regard, Atg4 members have differential substrate specificities. For example, Atg4A mainly cleaves GATE-16, whereas Atg4D cleaves both GATE-16 and GABARAP-L1.[20,22] Thus, GATE-16-PLA_2 fusion protein may provide a suitable substrate for Atg4A and Atg4D assay development. Indeed, we have generated and successfully tested a GATE-16-PLA_2 fusion protein for measuring activity of recombinant Atg4A,[19] using essentially the same assay conditions reported here (data not shown).

After counterscreening and elimination of false positives using a PLA_2 counterscreen, 4 compounds were identified from among 3280 bioactive molecules, showing concentration-dependent inhibitory activity (IC_{50} <10 μM) against Atg4B but not an alternative class of cysteine protease, caspase-3. Further testing using our autophagin-1 HTS assay in the presence or absence of DTT eliminated 2 compounds (1504078 and 1504080) that showed additive inhibition in the presence of DTT, indicating that hydrogen superoxide generation in vitro may be partially involved in inhibition of Atg4B.[29,30] Three of the compounds (1502245, 1504078, and 1504080) are also reported hits in other HTS assays reported in the PubChem database, whereas another compound (201508) inhibits Shp2 tyrosine phosphatase,[33] showing promiscuous activity. In addition, these compounds have structures that are not promising for lead optimization, with 2 compounds representing polyphenols containing carboxylates (with or without internal cyclization to form lactone rings; 201508, 1502245) and 2 compounds representing stereoisomers of a natural product senoside glycosylated with pyranose sugars (1504078 and 1504080). Although none of these compounds is an attractive candidate for undertaking structure-activity relation (SAR) studies toward potent and selective autophagin inhibitors, these pilot screening results nevertheless provide proof-of-concept evidence that the HTS assay described here is capable of identifying compounds with the potential for selectivity against autophagins relative to other classes of cysteine proteases.

Autophagy plays cytoprotective roles in some cancer-relevant contexts.[29,30,32] In this regard, inhibition of autophagy has been reported to sensitize some tumor cells to chemotherapy, suggesting that chemical inhibitors of autophagins may provide novel candidates for cancer drug discovery. Silencing Atg5 or Atg7 enhances apoptosis in chronic myeloid leukemia (CML) cells treated with imatinib mesylate (IM).[34] Autophagy inhibitor, 3-MA, or siRNA against Atg7 also augments 5-fluorouracil (5-FU)–induced apoptosis in colon cancer cells in vitro and in vivo.[35] Inhibiting autophagy with the nonselective PI3K inhibitor wortmannin (which crossreacts on the class III PI3K of autophagy, Vps34), as well as siRNAs targeting Vps34, Beclin1, or Atg5, appears to be synergistic with gossypol, a natural product that inhibits Bcl-2 family proteins, in human breast cancer cell MCF-7.[36] In these cancer cell culture models, inhibition of autophagy synergizes with cytotoxic anticancer drugs, and thus it has been suggested that autophagy allows cancer cells to survive the stress of chemotherapy. Thus, we anticipate that Atg4B-specific inhibitors may have tumor growth inhibitory activity, as well as an ability to improve cytotoxic responses to chemotherapy. It is hoped that applications of the HTS assay reported here for screening large compound libraries will provide attractive chemical scaffolds for the pursuit of a novel class of anticancer agents based on inhibition of autophagy.

ACKNOWLEDGMENTS

This work was supported by grants from National Institutes of Health (R01-AI-082629, R03-MH-090871, U54HG005033) and a fellowship grant to Dr. Shu from the SASS foundation for Medical Research (Rosyln, NY). We thank Tessa Siegfried and Melanie Hanaii for manuscript preparation.

REFERENCES

1. Marx J: Autophagy: is it cancer's friend or foe? *Science* 2006;312:1160-1161.
2. Mizushima N, Levine B, Cuervo AM, Klionsky DJ: Autophagy fights disease through cellular self-digestion. *Nature* 2008;451:1069-1075.
3. Todde V, Veenhuis M, van der Klei IJ: Autophagy: principles and significance in health and disease. *Biochim Biophys Acta* 2009;1792:3-13.
4. Reggiori F, Klionsky DJ: Autophagy in the eukaryotic cell. *Eukaryot Cell* 2002;1:11-21.
5. Nakatogawa H, Suzuki K, Kamada Y, Ohsumi Y: Dynamics and diversity in autophagy mechanisms: lessons from yeast. *Nat Rev Mol Cell Biol* 2009;10:458-467.
6. Tsukada M, Ohsumi Y: Isolation and characterization of autophagy-defective mutants of Saccharomyces cerevisiae. *FEBS Lett* 1993;333:169-174.
7. Jeong H, Then F, Melia TJ Jr, Mazzulli JR, Cui L, Savas JN, et al: Acetylation targets mutant huntingtin to autophagosomes for degradation. *Cell* 2009;137:60-72.

8. Olzmann JA, Chin LS: Parkin-mediated K63-linked polyubiquitination: a signal for targeting misfolded proteins to the aggresome-autophagy pathway. *Autophagy* 2008;4:85-87.
9. Chaumorcel M, Souquere S, Pierron G, Codogno P, Esclatine A. Human cytomegalovirus controls a new autophagy-dependent cellular antiviral defense mechanism. *Autophagy* 2008;4:46-53.
10. Jia K, Thomas C, Akbar M, Sun Q, Adams-Huet B, Gilpin C, et al: Autophagy genes protect against *Salmonella typhimurium* infection and mediate insulin signaling-regulated pathogen resistance. *Proc Natl Acad Sci U S A* 2009;106:14564-14569.
11. Mathew R, Karantza-Wadsworth V, White E: Role of autophagy in cancer. *Nat Rev Cancer* 2007;7:961-967.
12. Bommareddy A, Hahm ER, Xiao D, Powolny AA, Fisher AL, Jiang Y, et al: Atg5 regulates phenethyl isothiocyanate-induced autophagic and apoptotic cell death in human prostate cancer cells. *Cancer Res* 2009;69: 3704-3712.
13. Seglen PO, Gordon PB: 3-Methyladenine: specific inhibitor of autophagic/lysosomal protein degradation in isolated rat hepatocytes. *Proc Natl Acad Sci U S A* 1982;79:1889-1892.
14. Klionsky DJ, Elazar Z, Seglen PO, Rubinsztein DC: Does bafilomycin A1 block the fusion of autophagosomes with lysosomes? *Autophagy* 2008;4:849-950.
15. Barth S, Glick D, Macleod KF: Autophagy: assays and artifacts. *J Pathol* 2010;221:117-124.
16. Marino G, Uria JA, Puente XS, Quesada V, Bordallo J, Lopez-Otin C: Human autophagins, a family of cysteine proteinases potentially implicated in cell degradation by autophagy. *J Biol Chem* 2003;278:3671-3678.
17. Nakatogawa H, Ichimura Y, Ohsumi Y: Atg8, a ubiquitin-like protein required for autophagosome formation, mediates membrane tethering and hemifusion. *Cell* 2007;130:165-178.
18. Kirisako T, Baba M, Ishihara N, Miyazawa K, Ohsumi M, Yoshimori T, et al: Formation process of autophagosome is traced with Apg8/Aut7p in yeast. *J Cell Biol* 1999;147:435-446.
19. Shu CW, Drag M, Bekes M, Zhai D, Salvesen GS, Reed JC: Synthetic substrates for measuring activity of autophagy proteases—autophagins (Atg4). *Autophagy* 2010;6:936-947.
20. Betin VM, Lane JD: Caspase cleavage of Atg4D stimulates GABARAP-L1 processing and triggers mitochondrial targeting and apoptosis. *J Cell Sci* 2009;122:2554-2566.
21. Marino G, Fernandez AF, Cabrera S, Lundberg YW, Cabanillas R, Rodriguez F, et al: Autophagy is essential for mouse sense of balance. *J Clin Invest* 2010;120:2331-2344.
22. Scherz-Shouval R, Shvets E, Fass E, Shorer H, Gil L, Elazar Z: Reactive oxygen species are essential for autophagy and specifically regulate the activity of Atg4. *Embo J* 2007;26:1749-1760.
23. Marino G, Salvador-Montoliu N, Fueyo A, Knecht E, Mizushima N, Lopez-Otin C: Tissue-specific autophagy alterations and increased tumorigenesis in mice deficient in Atg4C/autophagin-3. *J Biol Chem* 2007;282:18573-18583.
24. Stennicke HR, Salvesen GS: Biochemical characteristics of caspases-3, -6, -7, and -8. *J Biol Chem* 1997;272:25719-25723.
25. Schimmer AD, Welsh K, Pinilla C, Wang Z, Krajewska M, Bonneau MJ, et al: Small-molecule antagonists of apoptosis suppressor XIAP exhibit broad antitumor activity. *Cancer Cell* 2004;5:25-35.
26. Nicholson B, Leach CA, Goldenberg SJ, Francis DM, Kodrasov MP, Tian X, et al: Characterization of ubiquitin and ubiquitin-like-protein isopeptidase activities. *Protein Sci* 2008;17:1035-1043.
27. Zhang JH, Chung TD, Oldenburg KR: A simple statistical parameter for use in evaluation and validation of high throughput screening assays. *J Biomol Screen* 1999;4:67-73.
28. Dijkstra BW, Drenth J, Kalk KH: Active site and catalytic mechanism of phospholipase A2. *Nature* 1981;289:604-606.
29. Soares KM, Blackmon N, Shun TY, Shinde SN, Takyi HK, Wipf P, et al: Profiling the NIH Small Molecule Repository for compounds that generate H202 by redox cycling in reducing environments. *Assay Drug Dev Technol* 2010;8:152-174.
30. Bova MP, Mattson MN, Vasile S, Tam D, Holsinger L, Bremer M, et al: The oxidative mechanism of action of ortho-quinone inhibitors of protein-tyrosine phosphatase alpha is mediated by hydrogen peroxide. *Arch Biochem Biophys* 2004;429:30-41.
31. Till A, Subramani S: A balancing act for autophagin. *J Clin Invest* 2010;120:2273-2276.
32. Satoo K, Noda NN, Kumeta H, Fujioka Y, Mizushima N, Ohsumi Y, et al: The structure of Atg4B-LC3 complex reveals the mechanism of LC3 processing and delipidation during autophagy. *Embo J* 2009;28:1341-1350.
33. Wu D, Pang Y, Ke Y, Yu J, He Z, Tautz L, et al: A conserved mechanism for control of human and mouse embryonic stem cell pluripotency and differentiation by shp2 tyrosine phosphatase. *PLoS One* 2009;4:e4914.
34. Bellodi C, Lidonnici MR, Hamilton A, Helgason GV, Soliera AR, Ronchetti M, et al: Targeting autophagy potentiates tyrosine kinase inhibitor-induced cell death in Philadelphia chromosome-positive cells, including primary CML stem cells. *J Clin Invest* 2009;119:1109-1123.
35. Li J, Hou N, Faried A, Tsutsumi S, Kuwano H: Inhibition of autophagy augments 5-fluorouracil chemotherapy in human colon cancer in vitro and in vivo model. *Eur J Cancer* 2010;46:1900-1909.
36. Gao P, Bauvy C, Souquere S, Tonelli G, Liu L, Zhu Y, et al: The BH3-mimetic gossypol induces both beclin 1–dependent and beclin 1–independent cytoprotective autophagy in cancer cells. *J Biol Chem* 2010;285:25570-25581.

Address correspondence to:
John C. Reed
Sanford-Burnham Medical Research Institute
10901 North Torrey Pines Road
La Jolla, CA 92037

E-mail: reedoffice@sanfordburnham.org